Hammondia hammondi, an avirulent relative of *Toxoplasma gondii*, has functional orthologs of known *T. gondii* virulence genes

Katelyn A. Walzer[a], Yaw Adomako-Ankomah[a], Rachel A. Dam[a], Daland C. Herrmann[b], Gereon Schares[b], Jitender P. Dubey[c,1], and Jon P. Boyle[a,1]

[a]Department of Biological Sciences, Dietrich School of Arts and Sciences, University of Pittsburgh, Pittsburgh, PA 15260; [b]Institute of Epidemiology, Friedrich-Loeffler-Institut, Federal Research Institute for Animal Health, D-16868 Wusterhausen, Germany; and [c]Animal Parasitic Diseases Laboratory, Beltsville Agricultural Research Center, Agricultural Research Service, US Department of Agriculture, Beltsville, MD 20705

Contributed by Jitender P. Dubey, March 8, 2013 (sent for review August 13, 2012)

Toxoplasma gondii **is a ubiquitous protozoan parasite capable of infecting all warm-blooded animals, including humans. Its closest extant relative,** ***Hammondia hammondi,*** **has never been found to infect humans and, in contrast to** ***T. gondii*****, is highly attenuated in mice. To better understand the genetic bases for these phenotypic differences, we sequenced the genome of a** ***H. hammondi*** **isolate (HhCatGer041) and found the genomic synteny between** ***H. hammondi*** **and** ***T. gondii*** **to be >95%. We used this genome to determine the** ***H. hammondi*** **primary sequence of two major** ***T. gondii*** **mouse virulence genes,** ***TgROP5*** **and** ***TgROP18*****. When we expressed these genes in** ***T. gondii*****, we found that** ***H. hammondi*** **orthologs of TgROP5 and TgROP18 were functional. Similar to** ***T. gondii*****, the** ***HhROP5*** **locus is expanded, and two distinct HhROP5 paralogs increased the virulence of a** ***T. gondii TgROP5*** **knockout strain. We also identified a 107 base pair promoter region, absent only in type III** ***TgROP18*****, which is necessary for TgROP18 expression. This result indicates that the** ***ROP18*** **promoter was active in the most recent common ancestor of these two species and that it was subsequently inactivated in progenitors of the type III lineage. Overall, these data suggest that the virulence differences between these species are not solely due to the functionality of these key virulence factors. This study provides evidence that other mechanisms, such as differences in gene expression or the lack of currently uncharacterized virulence factors, may underlie the phenotypic differences between these species.**

comparative genomics | gene content versus gene deployment | pathogenesis | host range

Approximately 20% of the US population is infected with the intracellular parasite *Toxoplasma gondii* (1). *T. gondii* is a member of the phylum Apicomplexa, which includes multiple human and animal pathogens, including the causative agents of malaria and cryptosporidiosis. A unique feature of this parasite compared with its apicomplexan relatives is the ability to infect, and cause disease in, nearly all warm-blooded animals studied to date, including birds (2). *T. gondii* is primarily asymptomatic in healthy humans but can cause severe disease in utero, in the immunocompromised, and in healthy adults (3–5). In the laboratory, the mouse model of toxoplasmosis has been extensively studied, a relevant model given that rodents are hosts for *T. gondii* in both rural and urban environments (6, 7). Highly virulent infections with *T. gondii* can be initiated by inoculation with fast-growing tachyzoites, slow-growing bradyzoite tissue stages (8), and oocysts (2). Felines are the definitive (i.e., sexual) host for *T. gondii* (9), and rodent to cat transmission via predation can expand the parasite population by up to 10 million-fold.

The closest extant relative of *T. gondii* is *Hammondia hammondi* (10, 11), a fellow apicomplexan that also has its sexual cycle in cats (10). This parasite was once thought to be a strain of *T. gondii* (12), but it is now accepted as a distinct species (2). Experimentally, a variety of intermediate hosts have been successfully infected with *H. hammondi* (including rabbits, pigs, rodents, and monkeys), but birds are refractory to infection (ref. 13, and reviewed in ref. 2). In contrast to *T. gondii*, in both wild-type and IFN-γ knockout mice, parenteral *H. hammondi* infections with all parasite life stages are nonlethal (2), although oral infections with high numbers of *H. hammondi* oocysts of some strains can cause disease (2) and mortality (13). In infected mice, *H. hammondi* tachyzoites and cysts can be found in several tissues, including lymph nodes and spleen (2). Importantly, *H. hammondi* tissue cysts (bradyzoites) from intermediate hosts are not infective to mice by any route, and therefore horizontal transmission between intermediate hosts is a unique feature of *T. gondii* (2, 13).

Why some humans become sick from *T. gondii* infection whereas most remain asymptomatic is largely unknown. Recently, attention has been focused on the genetic basis of parasite virulence, and mice have been used as a model for virulence in *T. gondii*. Among the virulence determinants, the most potent are rhoptry proteins 18 and 5 (TgROP18 and TgROP5), both members of a large superfamily of proteins secreted from parasite organelles called rhoptries (14–17). Subsequent work has shown that TgROP18 directly phosphorylates immune-related GTPases (IRGs) ,which prevents them from being efficiently loaded onto, and disrupting, the parasitophorous vacuole (PV) (18–24). For *TgROP5*, complete knockout of this locus in the hypervirulent type I strain renders the parasite completely avirulent in mice (15, 16), and this phenotype is due, at least in part, to ROP5 binding directly to IRG proteins, which presumably then permits TgROP18 IRG phosphorylation and inactivation (23, 24). Based on recent sequence analysis of the *Neospora caninum* genome [a parasite structurally similar to *T. gondii* but with a sexual cycle in dogs (25, 26)], it has been suggested that the orthologs of TgROP18 and TgROP5 are not functional as virulence genes in this species. Specifically, *ROP18* is a pseudogene in *N. caninum* (25), and the *NcROP5* locus has not significantly expanded in this species as it has in *T. gondii*, having only 2 copies compared with 4–10 in *T. gondii* (15, 16, 25). In addition, the *N. caninum* ROP18 ortholog has a similar promoter structure as the "avirulent" *TgROP18* allele in *T. gondii* strains with low *TgROP18* transcript abundance (27).

Author contributions: K.A.W., Y.A.-A., and J.P.B. designed research; K.A.W., Y.A.-A., R.A.D., D.C.H., G.S., J.P.D., and J.P.B. performed research; D.C.H., G.S., and J.P.D. contributed new reagents/analytic tools; K.A.W., Y.A.-A., and J.P.B. analyzed data; and K.A.W., D.C.H., G.S., J.P.D., and J.P.B. wrote the paper.

The authors declare no conflict of interest.

Data deposition: The HhCatGer041 genomic assembly and raw sequence reads have been deposited in GenBank under BioProject PRJNA191036 and BioSample 1974510.

[1]To whom correspondence may be addressed. E-mail: jitender.dubey@ars.usda.gov or boylej@pitt.edu.

This article contains supporting information online at www.pnas.org/lookup/suppl/doi:10.1073/pnas.1304322110/-/DCSupplemental.

The genetic bases for the dramatic differences in mouse virulence between *T. gondii* and *H. hammondi* are unknown. The goal of the present study was to sequence the genome of *H. hammondi* strain HhCatGer041 and use it to determine the overall degree of genomic identity and synteny between HhCatGer041 and *T. gondii*. We then functionally characterized the *H. hammondi* orthologs of TgROP18 and TgROP5 (HhROP18 and HhROP5) to determine whether they could be linked, or not, to the phenotypic differences between these closely related species.

Results

***H. hammondi* Genome Has High Synteny and Similarity to That of *T. gondii*.** Based on previously published analyses of internal transcribed spacer sequences (11, 28), *H. hammondi* has been categorized as the nearest extant relative of *T. gondii*, and our rough draft of the *H. hammondi* genome confirms this similarity. Details about the sequence reads and assembly are in Tables S1and S2. The genome assembled into 56,472 scaffolds, with the largest being 81 kb. When reads were mapped to the v7.2 draft of the *T. gondii* genome (strain GT1; www.toxodb.org), average coverage for nucleotides with >3× coverage was ~20×, and 68% of the GT1 nucleotides had ≥4× coverage (Fig. S1). Based on these alignments, the overall divergence genome-wide is 4.9%. The largest region without any sequence coverage was found on the first 175 kb of *T. gondii* Chr IX (Fig. S1). Despite its incomplete nature, the assembly provides strong evidence for a high degree of genomic synteny between these species. Specifically, strict reciprocal BLAST analysis of all predicted *T. gondii* coding regions (including introns) on 87 contigs >20 kb in length shows that 298 of 311 genes (~96%) are in the same order and orientation as they are in *T. gondii*. Importantly, only 96 genes (out of 8,993 queried) had no significant reciprocal blast hits ($E < 1e^{-5}$; Dataset S1). An identical comparison with *N. caninum* genes shows that 818 out of 7,226 predicted genes have no reciprocal blast hits [although more robust estimates of shared gene content between *T. gondii* and *N. caninum* have been published by others (25)]. Whereas the number of genes "missing" in *H. hammondi* compared with *T. gondii* will change as better assemblies of the *H. hammondi* genome emerge, this rough draft further establishes *H. hammondi* as the closest extant relative of *T. gondii* and sets the stage for gene-by-gene comparisons to better understand the evolution of virulence in *T. gondii*.

***ROP5* Locus Is Expanded, Diversified, and Functionally Conserved In *H. hammondi*.** Recently we and others demonstrated a clear role for the *TgROP5* locus in *T. gondii* virulence (15, 16). This locus was characterized by the presence of multiple paralogs that show clear evidence for selection-driven diversification (15). Using the *H. hammondi* genome sequence, we examined sequence read coverage on scaffolds with *H. hammondi ROP5* sequence (Fig. 1*A*), and this analysis suggested that the *ROP5* locus is also expanded in *H. hammondi*, with an estimated copy number of 8–10. To determine whether the locus had also diversified, we PCR-amplified and sequenced eight HhROP5 paralogs and identified eight distinct protein coding sequences (Fig. 1*B*, Fig. S2*A*), confirming that this locus is expanded and diversified in *H. hammondi* as it is in *T. gondii* (all primers used in this study are listed in Table S3). This finding is in contrast to what has been reported in *N. caninum* (25) although the role of NcROP5 in mouse virulence has not been directly tested. All eight isoforms harbored the same sequence features and domains as TgROP5 orthologs, including predicted signal sequences, an amphipathic helical domain in the N terminus that mediates interaction with the PV in TgROP5 (29), and a clear pseudokinase domain (Fig. S2*A*). Selection analyses also revealed that these individual copies showed strong evidence for selection. For example, isoform 2–4 has a non-synonymous/synonymous substitution ratio (dN/dS) of >2.8 compared with isoforms 1–3, 1–4, and 1–5, suggesting not only that the *HhROP5* locus has expanded in *H. hammondi* but also that it has been under selection.

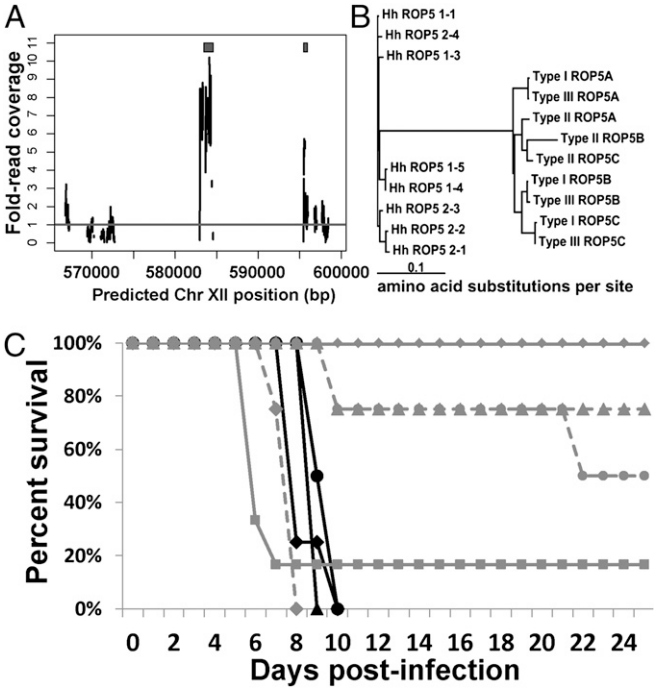

Fig. 1. Expansion, diversification, and functionality of *H. hammondi* ROP5. (*A*) Sequence coverage plot for three *H. hammondi* genomic scaffolds arranged based on their putative location on *H. hammondi* Chr XII (determined by Nucmer alignment of *H. hammondi* scaffolds to the v7.2 GT1 genome). Black blocks above the plots indicate the location of significant (expect < 1×10^{-10}) TBLASTN hits of TgROP5B against the *H. hammondi* genome. (*B*) Phylogram of amino acid sequences of eight HhROP5 paralogs and known TgROP5 paralogs. (*C*) Mice were infected with RH:WT (black lines) or RHΔ*ROP5* complemented with a single copy of either $HhROP5_{1–1}$ (gray solid lines) or $HhROP5_{2–1}$ (gray dashed lines). Four mice were used for each strain and dose with the exception of RHΔ*ROP5*:$HhROP5_{1–1}$ at 10^6 (n = 6), and RH:WT at 10^4 (n = 3). Tachyzoite dose symbol key: ■, 10^6; ◆, 10^5; ▲, 10^4; ●, 10^3.

Based on our sequence analyses of *HhROP5*, we chose two paralogs, 1–1 and 2–1 (Fig. 1*B*, Fig. S2*A*), for complementation into a type I *T. gondii* strain lacking the entire *TgROP5* locus [RHΔ*TgROP5* (15)]. In contrast to the parental strain (RH), which has an effective LD_{100} of a single parasite (30), this strain does not cause mortality at doses as high as 10^6 tachyzoites (15, 16). When expressed in *T. gondii*, HhROP5 paralogs 1–1 and 2–1 are both effectively trafficked to the *T. gondii* rhoptries (Fig. S3*B*) and can be found associated with the PV (Fig. S3*E*) as expected. Fusing 713 and 702 bp of upstream sequence from $HhROP5_{1–1}$ and $HhROP5_{2–1}$, respectively (Figs. S2*B* and S3*A*), with luciferase is capable of driving reporter expression at levels similar to one another and to a homologous upstream sequence for *T. gondii* type II *ROP5B* (Fig. S3*A*). In multiple experiments, it was found that the promoter activity of $HhROP5_{2–1}$ is slightly lower than $HhROP5_{1–1}$. Anti-HA Western blotting on parasites expressing these paralogs is consistent with this slight difference in promoter activity: normalized protein levels for $HhROP5_{2–1}$ are slightly lower than for $HhROP5_{1–1}$ (Fig. S3 *C* and *D*). To determine whether these HhROP5 orthologs were functionally conserved as virulence genes in *H. hammondi*, we infected mice with two genetically distinct clone sets of RHΔ*ROP5*:$ROP5Hh_{1–1}$ and RHΔ*ROP5*:$ROP5Hh_{2–1}$, along with RHΔROP5 and wild-type RH (Fig. S4*A*). For clone set 1, RHΔ*ROP5*:$ROP5Hh_{2–1}$ was 100% lethal at a dose of 10^5, and 50% lethal at a dose of 10^3

MICROBIOLOGY

(Fig. 1*C*). In contrast, RHΔ*ROP5*:ROP5Hh$_{1–1}$ was significantly less virulent than RHΔ*ROP5*:ROP5Hh$_{2–1}$, causing 80% mortality at a dose of 10^6 but none at lower doses (Fig. 1*C*). However, mice infected with RHΔ*ROP5*:ROP5Hh$_{1–1}$ did show signs of morbidity, in that mice infected with all doses (10^2 to 10^6) lost weight over the course of the infection (Fig. S4*B*). When a genetically distinct clone set was used to infect mice at doses of 10^5 and 10^4 tachyzoites, we observed similar differences in the efficacy of the *HhROP5* alleles (with the 2–1 allele being more effective at increasing the virulence of RHΔ*ROP5* than the 1–1 allele) although in these experiments both alleles conferred some lethality at doses as low as 10^4 tachyzoites (Fig. S4*C*). Regardless of the reasons for the differences in the results of these experiments with distinct clones, in both experiments, both the crude LD_{50} as well as the time to death at each dose was always shorter in mice infected with RHΔ*ROP5*:ROP5Hh$_{2–1}$ compared with RHΔ*ROP5*:ROP5Hh$_{1–1}$. Overall, these data show that *ROP5Hh$_{2–1}$* and *ROP5Hh$_{1–1}$* are functional virulence genes that are not equivalent in terms of their effects on mouse virulence when heterologously expressed in *T. gondii*.

***H. hammondi ROP18* Upstream Sequence Contains a 107-bp Core Promoter That Is Found Only in Active Tg*ROP18* Alleles.** The *H. hammondi ROP18* gene is structurally most similar to the avirulent type III *TgROP18*, both in its promoter and coding region (Fig. S5*A*). It has a promoter similar in length to type III *TgROP18*, whose promoter is inactive and four-to-five times longer than *T. gondii* type I and II ROP18 promoters (27, 31). This difference in promoter structure is due to a 2.1-kb insertion in the type III gene relative to types I and II, and a corresponding 201-bp deletion (27, 31). Surprisingly, when we placed the *H. hammondi ROP18* promoter sequence upstream of luciferase, we found that it is highly active in these assays, in direct contrast to the corresponding upstream sequence from type III Tg*ROP18* (Fig. 2*B*). This surprising result indicates that the 2.1-kb insertion itself is not the cause of reduced transcription of Tg*ROP18*, but rather some other promoter element. We have identified this element, which is a 107-bp deletion in the type III promoter compared with the *HhROP18* promoter (Fig. 2*A*). This region is present in both the type I and type II *TgROP18* alleles, and *H. hammondi*, just upstream of the predicted transcriptional start site (Fig. 2*A*). When this 107-bp region is deleted in the *HhROP18* promoter, it completely inactivates its activity in luciferase reporter assays (Fig. 2*B*, *Left*; raw values shown in Table S4). Additionally, when this 107-bp fragment is inserted into the type III strain *TgROP18* promoter, the presence of this sequence dramatically increases the activity of this promoter in reporter assays, increasing its activity by over eightfold compared with the type II *TgROP18* promoter (Fig. 2*B*, *Right*). Therefore, we conclude that this small upstream sequence plays a key role in HhROP18 expression in *H. hammondi* and suggests that it is similarly important in type I and type II strains of *T. gondii*.

***H. hammondi ROP18* Is a Highly Functional Virulence Gene in *T. gondii*.** To see whether *H. hammondi ROP18* is functional as a virulence gene, we complemented a type III strain with *HhROP18* or *TgROP18* from each of the three major *T. gondii* lineages (types I, II and III). As expected, HA-tagged TgROP18$_{II}$ and HhROP18 (Fig. 2*C*) all trafficked to the *T. gondii* rhoptries, and HA-tagged HhROP18 could also be found on the parasitophorous vacuolar membrane (PVM) (Fig. S5*D*). In contrast, and consistent with our promoter activity experiments (Fig. 2*B*), there was no visible HA staining in TgROP18$_{III}$-transfected parasites, despite the fact that the construct was present (Fig. S5*E*). To compare the impact of expression of these 4 *ROP18* alleles on parasite virulence, mice were infected intraperitoneally with 1,000 tachyzoites of III:EV (empty vector), III:TgROP18$_{I}$, III:TgROP18$_{II}$, III:TgROP18$_{III}$, and III:HhROP18, and parasite burden was assessed daily using in vivo bioluminescence imaging (BLI). As expected, mice infected with III:TgROP18$_{III}$ and III:EV did not succumb to the

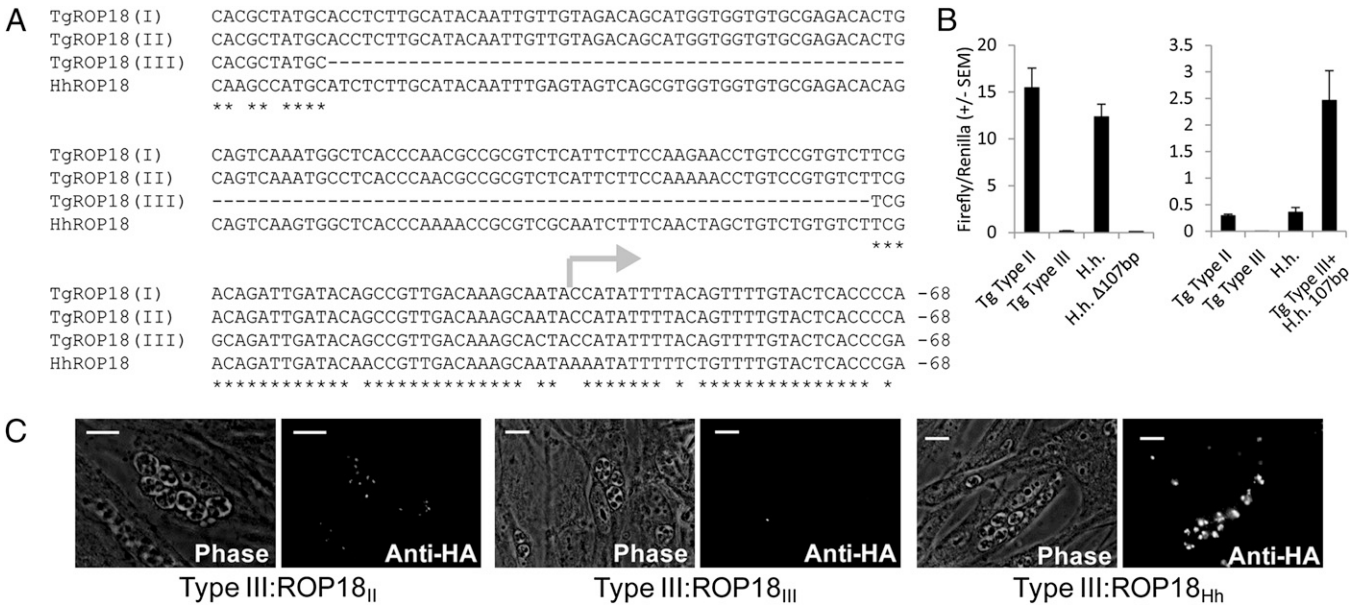

Fig. 2. A 107-bp region of the *H. hammondi* ROP18 promoter is necessary for gene expression. (*A*) Alignment of the *HhROP18* and *TgROP18$_{III}$* promoters just upstream of the transcriptional start site (gray arrow). Numbers represent nucleotide position relative to the start codon. (*B*) The *HhROP18* upstream sequence had promoter activity that was similar to *TgROP18$_{II}$* but significantly greater than *TgROP18$_{III}$*. Deletion of the 107-bp region present in *HhROP18* and types I and II *T. gondii* dramatically reduced promoter activity when assayed in *T. gondii*. Data for two luciferase assays are shown as the ratios of firefly luciferase signal to *Renilla* luciferase signal (*Left*). When this 107-bp fragment was introduced into the *TgROP18* type III upstream sequence, it dramatically increased the normalized luciferase signal compared with the type II and type III ROP18 promoter sequences (*Right*). (*C*) Anti-HA immunofluorescence showing the localization of TgROP18$_{II}$, TgROP18$_{III}$, and HhROP18 and lack of staining in the strains harboring TgROP18$_{III}$. (Scale bar: 10 μm.)

infection and showed comparatively low levels of parasite burden over the course of the infection (Fig. 3 *A*–*C*). All mice infected with III:TgROP18$_{I}$ and III:TgROP18$_{II}$ died by day 16 (Fig. 3*B*). Remarkably, >80% of mice infected with III:HhROP18 died before mice infected with any of the other strains, including those infected with III:TgROP18$_{I}$ (Fig. 3*B*). This difference in time to mortality is consistent with the in vivo BLI data. Specifically, III:HhROP18 increased in number in infected mice much more rapidly than all other strains, being over 10-fold higher than all other strains on days 6 and 7 postinfection (Fig. 3*A*). These data show that, despite being derived from a parasite species that is attenuated in mice, the *H. hammondi ROP18* gene, when expressed in *T. gondii*, may actually be a more effective virulence gene than the alleles from *T. gondii* types I and II. Based on quantitative Western blotting, HhROP18 is expressed at similar levels as TgROP18$_{I}$ (Fig. S5 *B* and *C*), suggesting that the *HhROP18* allele, rather than differences in expression level, are responsible for the increased impact of *HhROP18* on virulence compared with the *T. gondii ROP18* alleles from type I and type II strains.

Discussion

The differences in virulence between *H. hammondi* and *T. gondii* are belied by their close phylogenetic relationship. In contrast to *T. gondii*, when oocysts are injected subcutaneously or

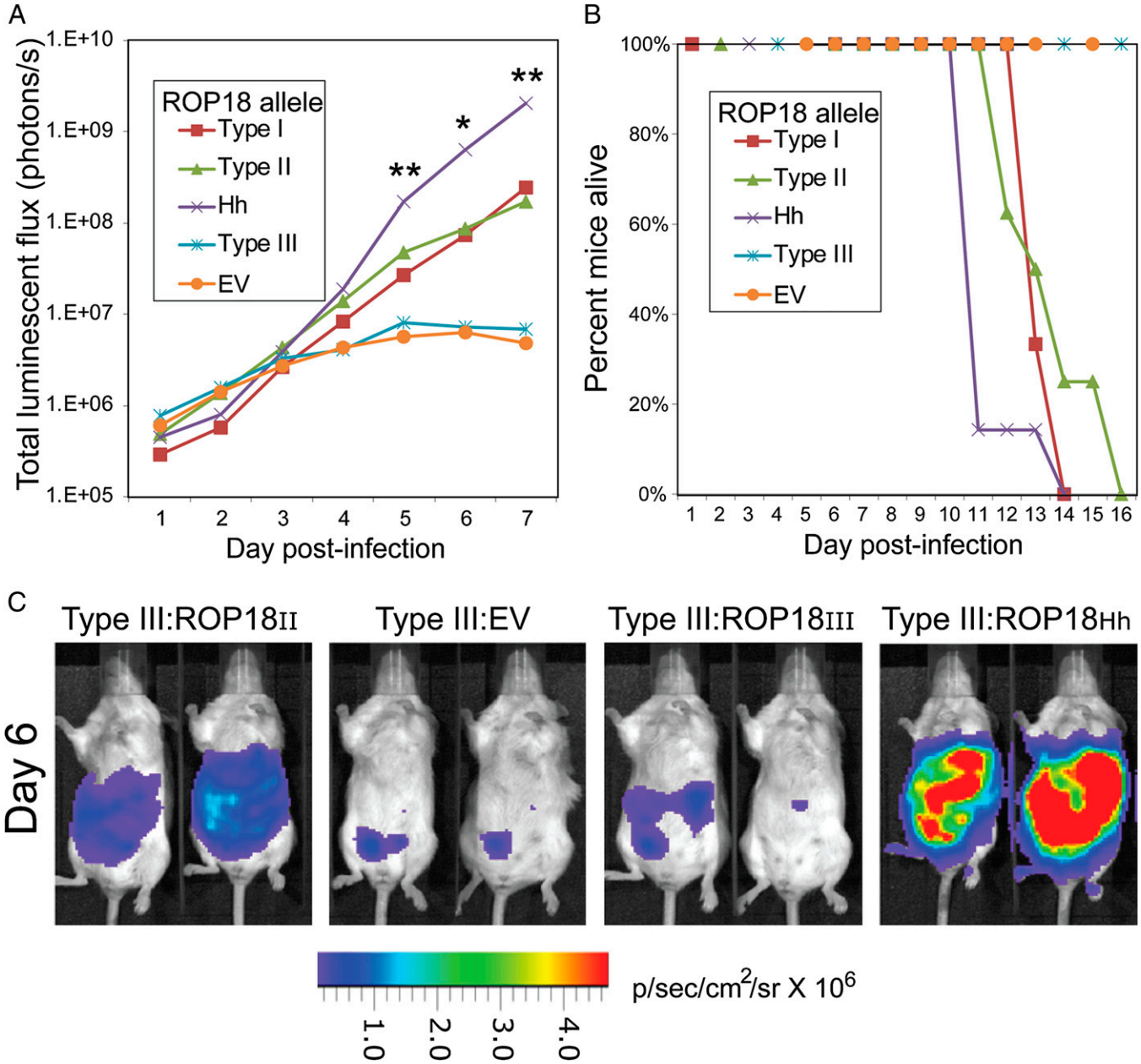

Fig. 3. Expressing HhROP18 in a TgType III background increases parasite lethality and in vivo proliferation. Mice were infected with 10^3 parasites of a type III strain complemented with TgROP18$_{I}$, TgROP18$_{II}$, TgROP18$_{III}$, HhROP18, or empty vector (n = 3, 8, 5, 7, and 5, respectively). Results shown are pooled from two experiments. (*A*) Quantitative in vivo BLI of infected mice. Asterisks indicate significantly higher luciferase signal in HhROP18-complemented parasites compared with TgROP18$_{I}$-complemented parasites (*P < 0.05; **P < 0.01). (*B*) Mouse mortality. (*C*) Representative images of parasite burden in mice on day 6 postinfection.

intraperitoneally, *H. hammondi* is completely avirulent in wild-type and IFN-γ knockout mice (2) and has never been found to infect humans. A number of mechanisms could explain the dramatic virulence differences between two species that share such a recent common ancestry. One is that virulence is driven by genes that are uniquely present and/or divergent in *T. gondii* compared with *H. hammondi*. Another is that both species harbor the same arsenal of effectors, but they are differentially regulated by distinct transcriptional mechanisms or transcription factors. However, another is that the *H. hammondi* genome contains "avirulence" genes that are only present and/or expressed in *H. hammondi*. Genome sequence comparison between these organisms is a crucial first step in addressing these hypotheses and to ultimately determine how mouse virulence, as well as other traits, evolved uniquely in *T. gondii*.

In the present study, we found that *H. hammondi* orthologs of *ROP5* and *ROP18*, which are the most potent mouse virulence factors known in *T. gondii* (14–17), are functional when expressed heterologously in *T. gondii*. As in *T. gondii*, the *HhROP5* locus has expanded, and individual paralogs appear to be under diversifying selection in *H. hammondi*. Specifically, *H. hammondi* $ROP5_{2–1}$ increases the virulence of a *T. gondii ROP5* knockout strain 100-fold, and this effect is more potent than complementation of the same ROP5 knockout strain with a single copy of *T. gondii ROP5* [the ROP5 "A"isoform (15)]. Whereas RHΔTg*ROP5*:TgROP5A was lethal to only 20% at a dose of 10^5 tachzyoites, we observed 100% mortality with this dose of RHΔTg*ROP5*:ROP5$Hh_{2–1}$, and 50% mortality at a dose of 1,000 RHΔTg*ROP5*:$Hh_{2–1}$ tachyzoites. Interestingly, in terms of mouse mortality, $HhROP5_{1–1}$ was less potent than $HhROP5_{2–1}$. Overall these data indicate that the *ROP5* locus in *H. hammondi* bears all of the hallmarks of the orthologous locus from *T. gondii*: (*i*) it contains multiple copies that have undergone selection-driven diversification in sequence, (*ii*) individual copies can increase the pathogenesis of a *T. gondii ROP5* knockout, and (*iii*) individual copies vary in terms of their effects on virulence. Interestingly, across the *H. hammondi ROP5* paralogs, the most polymorphic region is found within the pseudokinase domain in residues 490–501, and a similar level of polymorphism is found in this same region across the *T. gondii ROP5* paralogs (Fig. S2*A*) (15). Future work on the other six *H. hammondi ROP5* paralogs will provide more information on the impact of locus diversification in this species. Moreover, we have not yet tested the impact of expressing multiple distinct copies of *H. hammondi ROP5* orthologs, nor the impact of *H. hammondi ROP5* expression on the loading of IRG GTPases (23, 24). These studies should help to inform current models of TgROP5 structure-activity relationships in *T. gondii*.

In *T. gondii*, virulence gene expression, rather than individual amino acid polymorphisms, has been linked to differences in virulence between strains. Specifically, *TgROP18* transcript abundance in type III strains is significantly lower than in members of the type I and II lineages, and, within the *T. gondii* species, this lower transcript abundance is clearly due to a 2.1-kb sequence inserted 85 bp upstream of the ROP18 start codon compared to strain types I and II (27, 31). We found that a similarly homologous insertion was present in the *H. hammondi ROP18* upstream sequence. Given the presence of this insertion, we were surprised to find that, in contrast to the corresponding sequence from *T. gondii* type III strains, the *H. hammondi ROP18* promoter drove significantly high levels of luciferase in promoter assays conducted in *T. gondii*. We identified a 107-bp region in *H. hammondi* and type I and II *T. gondii ROP18* upstream of the predicted transcriptional start site that is not present in *T. gondii* type III *ROP18*. Deletion of this sequence in *H. hammondi ROP18* destroys promoter activity, suggesting that this sequence contains a core ROP18 promoter or enhancer element in both species (at least when heterologously expressed in *T. gondii*). Even more exciting, inserting this *H. hammondi* sequence into the comparatively ineffective type III promoter at the proper location effectively resurrects this promoter to levels that are even higher than the $TgROP18_{II}$ promoter. Importantly, based on BLASTN, this 107-bp sequence cannot be identified in the entire *N. caninum* genome (expect >10), suggesting that the *ROP18* promoter became "active" after the split between the *N. caninum* and *T. gondii*/*H. hammondi* lineages. This increased promoter activity has significant phenotypic consequence: HhROP18 appears to be at least as potent as, and possibly MORE potent than, $TgROP18_{I}$.

Through a preliminary sequence analysis of an isolate of *H. hammondi* (HhCatGer041), we have found that orthologs of key *T. gondii* mouse virulence genes are functionally conserved in this species. Whereas virulence commonly evolves in pathogenic bacteria by changes in gene content via acquisition of so-called pathogenicity islands [e.g., in pathogenic *Escherichia coli* (32)], in the case of the eukaryotic pathogens *T. gondii* and *H. hammondi*, at least, gene content and functionality may not be sufficient to explain their phenotypic differences. One hypothesis is that the inability of *H. hammondi* to infect and be transmitted by mice compared with *T. gondii* is due to differences in gene deployment. This explanation for the phenotypic differences between T. gondii and H. hammondi would be somewhat analogous to what has been found in transcriptome comparisons between free-living and "parasitic" forms of *Listeria monocytogenes* where highly distinct transcriptional profiles, driven by activation/deactivation of key transcription factors, are the hallmark of the pathogenic lifestyle (33). High quality data from the *H. hammondi* transcriptome will be necessary to address this hypothesis. Transcriptome analyses in *H. hammondi* are made more difficult by the fact that *H. hammondi* does not replicate for more than 5 d in cell culture and therefore must be generated directly from cat-derived oocyst stages. However, the depth of next generation sequencing provides a potential solution to this problem. These analyses will be facilitated by the crude *H. hammondi* genome draft presented here as well as the recently released draft of a different isolate (H.H.34) by the J. Craig Venter Institute (http://jcvi.org).

Methods

Parasite Strains and Maintenance. *T. gondii* parasites were allowed to invade monolayers of human foreskin fibroblasts (HFFs) that were grown at 37 °C in 5% CO_2. HFFs were maintained in Dulbecco's modified Eagle's medium with 10% (vol/vol) FCS, 2 mM glutamine, and 50 μg/mL each of penicillin and streptomycin (cDMEM). RH, ME49, and CEP were used as representative type I, II, and III strains, respectively. The *H. hammondi* strain (HhCatGer041) was isolated from cat feces on June 29, 2009 during a survey of *Toxoplasma gondii* in Germany. The isolate was confirmed as *Hammondia hammondi* as previously described (34) using specific *Hammondia hammondi* primers (35) and by the complete nonvirulence of the parasite in IFN-γ knockout mice. For *H. hammondi* oocyst production, IFN-γ knockout mice were fed 10^4 *H. hammondi* oocysts and killed 59 d later. Muscles from infected mice were fed to 10- to 20-wk-old cats, and feces were collected during days 5–11 postinfection. Unsporulated oocysts were isolated by sucrose floatation and allowed to sporulate at room temperature in 2% sulfuric acid (2).

DNA Isolation from *H. hammondi* Oocysts. Sporulated oocysts (40-80 million) were washed four times in Hanks' balanced salt solution (HBSS) and treated with 10% bleach in PBS for 30 min. Washed pellets were resuspended in 4 mL of HBSS in a 15-mL falcon tube, and 1 g of sterile glass beads (710-1,180 μM; Sigma) were added. Parasites were vortexed on high speed for 30 s, cooled for 30 s, and then vortexed for 30 s more. The supernatant was removed and pelleted by centrifugation. DNA was isolated from this preparation, which contained sporocysts that had been freed from the oocyst using the DNAzol reagent according to the manufacturer (Life Technologies). For two different preparations, 8 ng of DNA was linearly amplified using the GenomiPhi DNA Amplification Kit (GE Healthcare Life Sciences) and ethanol precipitated. These preparations were used for Illumina and PacBio *RS* (Pacific Biosciences) library preparation and sequencing and for PCR amplification (described in *Gene Identification, Sequencing, and Generation of Transgenic* T. gondii).

Sequencing, de Novo Assembly, and Analysis of the *H. hammondi* Genome. For Illumina sequencing, two different preparations of linearly amplified

H. hammondi DNA were combined, and a single library (insert size ~200 bp) was made from the preparation using the DNA TrueSeq kit. Thirty million 36-bp paired-end reads were generated in a single lane of an Illumina Genome Analyzer IIx at the Tufts Genomics Core Facility. Mean insert size and SD were calculated via de novo assembly in Ray (36). Two additional linearly amplified DNA samples were combined and submitted to the Duke Genomics Core Facility, and sequence data from four single molecule, real-time (SMRT) cells were obtained from a 2-kb insert library on a PacBio *RS* system. Consensus PacBio *RS* reads were assembled along with the Illumina reads using Ray with the following settings: K-mer size of 21, a mean insert size of 206, and a SD of 33. The K-mer size was determined iteratively by running the assembly using K-mer sizes ranging from 12 to 23 to maximize the N50 value. Synteny analyses were performed by reciprocal BLASTN between the genomic DNA coding regions for all v7.2 ME49 predicted genes versus the *H. hammondi* genomic contigs with an expected value of $1e^{-5}$. Genes on contigs larger than 20 kb were then scored manually for reciprocal hit presence, order, and orientation. Raw Illumina sequence reads were aligned to the v7.2 GT1 *T. gondii* genome using Bowtie2 (http://bowtie-bio.sourceforge.net/bowtie2/index.shtml) using the following parameters: bowtie2 –local -L 10 -k 10 -i S,1,0.5. Coverage plots were generated using Samtools mpileup on the bowtie2 output, and coverage was determined at each base using a custom perl script.

Gene Identification, Sequencing, and Generation of Transgenic *T. gondii*. *H. hammondi* contigs with *ROP5* and *ROP18* coding and upstream sequences were identified using TBLASTN with *T. gondii* ROP5 and ROP18 protein sequences. HhROP5 isoforms were PCR amplified using short-cycle, long-extension PCR to amplify ~1,000 bp upstream of the predicted start codon to the predicted stop codon (Invitrogen). Eight distinct clones were sequenced and protein sequences aligned using CLUSTALW (37). Two paralogs (1-1 and 2-1) were amplified directly from the cloning plasmid (PCR2.1 TOPO) using primers with AscI (Forward) and XmaI (Reverse) sites and cloned into the pUPRT-HA vector (15) in frame with an HA tag. Selection for plasmid integration into RHΔTg*ROP5* was performed using 5-fluorodeoxyuridine (38), and resistant parasites were cloned by limiting dilution. Sequences for *Hh, Tg_I, Tg_{II},* and *Tg_{III} ROP18* were directionally cloned into pENTR-D-Topo (Invitrogen) and recombined into a derivative of the pGRA-HA-HPT vector (14) in which the *Gra1* upstream sequence was replaced with the *attR1-ccdB-attR2* cassette for Gateway recombination cloning (Invitrogen) (39, 40). The constructs were transfected into a click beetle luciferase-expressing *T. gondii* strain null for HXGPRT (CEP) (14). Parasites were selected for resistance to mycophenolic acid and xanthine and cloned by limiting dilution (41). PCR was used to verify the presence of the full construct in III:*$TgROP18_{III}$* parasites. All clones were validated using anti-HA immunofluorescence and Western blotting. Primers are listed in Table S3.

ACKNOWLEDGMENTS. We thank Michael Reese for helpful comments on the manuscript. This work was supported by a Pew Scholarship in the Biomedical Sciences and by National Institute of Allergy and Infectious Diseases K22 Research Scholar Award 5K22AI080977 (to J.P.B.), and by Howard Hughes Medical Institute-sponsored undergraduate research fellowships (to K.A.W. and R.A.D.). D.C.H. and G.S. were supported by German Federal Ministry of Education and Research Grants 01 KI 0765, Toxonet01 and 01 KI 1002 F, Toxonet02.

1. Jones JL, et al. (2001) *Toxoplasma gondii* infection in the United States: Seroprevalence and risk factors. *Am J Epidemiol* 154(4):357–365.
2. Dubey JP, Sreekumar C (2003) Redescription of *Hammondia hammondi* and its differentiation from *Toxoplasma gondii*. *Int J Parasitol* 33(13):1437–1453.
3. Luft BJ, et al. (1993) Toxoplasmic encephalitis in patients with the acquired immunodeficiency syndrome. *N Engl J Med* 329(14):995–1000.
4. Remington JS, Klein JO (2001) *Infectious Diseases of the Fetus and Newborn Infant* (Saunders, Philadelphia), 5th Ed.
5. Carme B, Demar M, Ajzenberg D, Dardé ML (2009) Severe acquired toxoplasmosis caused by wild cycle of *Toxoplasma gondii*, French Guiana. *Emerg Infect Dis* 15(4): 656–658.
6. Kijlstra A, et al. (2008) The role of rodents and shrews in the transmission of *Toxoplasma gondii* to pigs. *Vet Parasitol* 156(3-4):183–190.
7. Murphy RG, et al. (2008) The urban house mouse (Mus domesticus) as a reservoir of infection for the human parasite *Toxoplasma gondii*: An unrecognised public health issue? *Int J Environ Health Res* 18(3):177–185.
8. Boyle JP, Saeij JP, Boothroyd JC (2007) *Toxoplasma gondii*: Inconsistent dissemination patterns following oral infection in mice. *Exp Parasitol* 116(3):302–305.
9. Frenkel JK, Dubey JP, Miller NL (1970) *Toxoplasma gondii* in cats: Fecal stages identified as coccidian oocysts. *Science* 167(3919):893–896.
10. Frenkel JK, Dubey JP (1975) *Hammondia hammondi*: A new coccidium of cats producing cysts in muscle of other mammals. *Science* 189(4198):222–224.
11. Su C, et al. (2003) Recent expansion of *Toxoplasma* through enhanced oral transmission. *Science* 299(5605):414–416.
12. Heydorn AO, Mehlhorn H (2001) Further remarks on *Hammondia hammondi* and the taxonomic importance of obligate heteroxeny. *Parasitol Res* 87(7):573–577.
13. Frenkel JK, Dubey JP (1975) *Hammondia hammondi* gen. nov., sp.nov., from domestic cats, a new coccidian related to *Toxoplasma* and *Sarcocystis*. *Z Parasitenkd* 46(1):3–12.
14. Saeij JP, et al. (2006) Polymorphic secreted kinases are key virulence factors in toxoplasmosis. *Science* 314(5806):1780–1783.
15. Reese ML, Zeiner GM, Saeij JP, Boothroyd JC, Boyle JP (2011) Polymorphic family of injected pseudokinases is paramount in *Toxoplasma* virulence. *Proc Natl Acad Sci USA* 108(23):9625–9630.
16. Behnke MS, et al. (2011) Virulence differences in *Toxoplasma* mediated by amplification of a family of polymorphic pseudokinases. *Proc Natl Acad Sci USA* 108(23): 9631–9636.
17. Taylor S, et al. (2006) A secreted serine-threonine kinase determines virulence in the eukaryotic pathogen *Toxoplasma gondii*. *Science* 314(5806):1776–1780.
18. Pawlowski N, et al. (2011) The activation mechanism of Irga6, an interferon-inducible GTPase contributing to mouse resistance against *Toxoplasma gondii*. *BMC Biol* 9:7.
19. Steinfeldt T, et al. (2010) Phosphorylation of mouse immunity-related GTPase (IRG) resistance proteins is an evasion strategy for virulent *Toxoplasma gondii*. *PLoS Biol* 8(12):e1000576.
20. Khaminets A, et al. (2010) Coordinated loading of IRG resistance GTPases on to the *Toxoplasma gondii* parasitophorous vacuole. *Cell Microbiol* 12(7):939–961.
21. Zhao YO, Khaminets A, Hunn JP, Howard JC (2009) Disruption of the *Toxoplasma gondii* parasitophorous vacuole by IFNgamma-inducible immunity-related GTPases (IRG proteins) triggers necrotic cell death. *PLoS Pathog* 5(2):e1000288.
22. Martens S, et al. (2005) Disruption of *Toxoplasma gondii* parasitophorous vacuoles by the mouse p47-resistance GTPases. *PLoS Pathog* 1(3):e24.
23. Niedelman W, et al. (2012) The rhoptry proteins ROP18 and ROP5 mediate *Toxoplasma gondii* evasion of the murine, but not the human, interferon-gamma response. *PLoS Pathog* 8(6):e1002784.
24. Fleckenstein MC, et al. (2012) A *Toxoplasma gondii* pseudokinase inhibits host IRG resistance proteins. *PLoS Biol* 10(7):e1001358.
25. Reid AJ, et al. (2012) Comparative genomics of the apicomplexan parasites *Toxoplasma gondii* and *Neospora caninum*: Coccidia differing in host range and transmission strategy. *PLoS Pathog* 8(3):e1002567.
26. Collantes-Fernandez E, et al. (2012) Infected dendritic cells facilitate systemic dissemination and transplacental passage of the obligate intracellular parasite *Neospora caninum* in mice. *PLoS ONE* 7(3):e32123.
27. Khan A, Taylor S, Ajioka JW, Rosenthal BM, Sibley LD (2009) Selection at a single locus leads to widespread expansion of *Toxoplasma gondii* lineages that are virulent in mice. *PLoS Genet* 5(3):e1000404.
28. Ellis JT, et al. (1999) The genus *Hammondia* is paraphyletic. *Parasitology* 118(Pt 4): 357–362.
29. Reese ML, Boothroyd JC (2009) A helical membrane-binding domain targets the *Toxoplasma* ROP2 family to the parasitophorous vacuole. *Traffic* 10(10):1458–1470.
30. Sibley LD, Boothroyd JC (1992) Virulent strains of *Toxoplasma gondii* comprise a single clonal lineage. *Nature* 359(6390):82–85.
31. Boyle JP, Saeij JP, Harada SY, Ajioka JW, Boothroyd JC (2008) Expression quantitative trait locus mapping of *toxoplasma* genes reveals multiple mechanisms for strain-specific differences in gene expression. *Eukaryot Cell* 7(8):1403–1414.
32. Perna NT, et al. (2001) Genome sequence of enterohaemorrhagic *Escherichia coli* O157:H7. *Nature* 409(6819):529–533.
33. Toledo-Arana A, et al. (2009) The *Listeria* transcriptional landscape from saprophytism to virulence. *Nature* 459(7249):950–956.
34. Herrmann DC, et al. (2010) Atypical *Toxoplasma gondii* genotypes identified in oocysts shed by cats in Germany. *Int J Parasitol* 40(3):285–292.
35. Schares G, et al. (2008) Characterization of a repetitive DNA fragment in *Hammondia hammondi* and its utility for the specific differentiation of *H. hammondi* from *Toxoplasma gondii* by PCR. *Mol Cell Probes* 22(4):244–251.
36. Boisvert S, Laviolette F, Corbeil J (2010) Ray: Simultaneous assembly of reads from a mix of high-throughput sequencing technologies. *J Comput Biol* 17(11):1519–1533.
37. Larkin MA, et al. (2007) Clustal W and Clustal X version 2.0. *Bioinformatics* 23(21): 2947–2948.
38. Donald RG, Roos DS (1995) Insertional mutagenesis and marker rescue in a protozoan parasite: Cloning of the uracil phosphoribosyltransferase locus from *Toxoplasma gondii*. *Proc Natl Acad Sci USA* 92(12):5749–5753.
39. Rosowski EE, et al. (2011) Strain-specific activation of the NF-kappaB pathway by GRA15, a novel *Toxoplasma gondii* dense granule protein. *J Exp Med* 208(1):195–212.
40. Hartley JL, Temple GF, Brasch MA (2000) DNA cloning using *in vitro* site-specific recombination. *Genome Res* 10(11):1788–1795.
41. Donald RG, Carter D, Ullman B, Roos DS (1996) Insertional tagging, cloning, and expression of the *Toxoplasma gondii* hypoxanthine-xanthine-guanine phosphoribosyltransferase gene. Use as a selectable marker for stable transformation. *J Biol Chem* 271(24):14010–14019.

Supporting Information

Walzer et al. 10.1073/pnas.1304322110

SI Methods

Immunofluorescence. Parasites were allowed to invade cell monolayers on coverslips for 18 or 24 h. The cells were washed once with PBS before fixation. In most cases, the cells were fixed with 4% formaldehyde for 20 min, washed twice in PBS, and blocked in PBS supplemented with 5% BSA and 0.2% Triton X-100. For parasite strains expressing GFP, fixation was performed with ice-cold methanol for 20 min. Antibodies used in this study are anti-SAG1 (GenWay), and secondary fluorescent antibodies (Invitrogen). Monoclonal antibodies to *T. gondii* ROP7 were provided by Peter Bradley (University of California, Los Angeles) (1), and rabbit polyclonal antibodies to *T. gondii* ROP18 and *T. gondii* ROP5 were provided by David Sibley (Washington University in St. Louis).

Western Blotting. Equal numbers of parasites ($\sim 1 \times 10^6$) expressing different HA-tagged constructs were solubilized in SDS/PAGE lysis buffer, and samples were run on 10% SDS/PAGE gels. Following transfer to nitrocellulose, blots were probed with a rat anti-HA monoclonal (clone 3F10; Roche) coupled to horseradish peroxidase (1:10,000 dilution) or a mouse polyclonal antibody against *T. gondii* SAG1 (1:10,000), followed by secondary staining with goat anti-mouse antibodies coupled to HRP (1:10,000). Bands were visualized using the Signal West Pico Chemiluminescence Kit (Pierce).

Promoter Activity Assays. Upstream sequences were PCR-amplified and directionally cloned into pENTR-D-Topo and then recombined into pDEST-Luc using the Gateway Cloning system as described previously (2). Constructs were transfected into *T. gondii* strain ME49B7 and analyzed 24 h posttransfection using dual luciferase assays as described (2). The following sequences upstream of the start codon were used: $HhROP5_{1–1}$ and $HhROP5_{2–1}$, 713 and 702 bp, respectively; $TgROP5_{II}$, 708 bp; and HhROP18 and $TgROP18_{I}$, $TgROP18_{II}$, and $TgROP18_{III}$, 633, 2,664 and 2,785 bp, respectively. Splicing by overlapping extension-PCR (3) was used to delete the putative core *HhROP18* promoter and to insert the putative core *HhROP18* promoter into the $TgROP18_{III}$ promoter. Primers are listed in Table S3.

Mouse Studies. Female BALB/c mice aged 4 to 21 wk (The Jackson Laboratory) were used in all in vivo experiments. Parasites were isolated from host cells by needle passage, washed once in PBS, and quantified, and mice were inoculated i.p. with a 28-gauge needle. Parasite viability was assessed using plaque assay (4). Mortality and mouse weight were assessed up to three times daily, and surviving mice were bled and tested for the presence of anti-*T. gondii* antibodies using immunofluorescence as described (5). For experiments with *HhROP18* and *TgROP18*-complemented *T. gondii*, parasite burden was assessed and analyzed daily using in vivo bioluminescence imaging (BLI) as described (6) using an IVIS Lumina II in vivo imaging system (Caliper Life Sciences). All animal protocols were approved by the Institutional Animal Care and Use Committee (IACUC) at the University of Pittsburgh.

1. Rome ME, Beck JR, Turetzky JM, Webster P, Bradley PJ (2008) Intervacuolar transport and unique topology of GRA14, a novel dense granule protein in *Toxoplasma gondii*. *Infect Immun* 76(11):4865–4875.
2. Boyle JP, Saeij JP, Harada SY, Ajioka JW, Boothroyd JC (2008) Expression quantitative trait locus mapping of *toxoplasma* genes reveals multiple mechanisms for strain-specific differences in gene expression. *Eukaryot Cell* 7(8):1403–1414.
3. Horton RM, Cai ZL, Ho SN, Pease LR (1990) Gene splicing by overlap extension: Tailor-made genes using the polymerase chain reaction. *Biotechniques* 8(5):528–535.
4. Reese ML, Zeiner GM, Saeij JP, Boothroyd JC, Boyle JP (2011) Polymorphic family of injected pseudokinases is paramount in *Toxoplasma* virulence. *Proc Natl Acad Sci USA* 108(23):9625–9630.
5. Saeij JP, et al. (2006) Polymorphic secreted kinases are key virulence factors in toxoplasmosis. *Science* 314(5806):1780–1783.
6. Saeij JP, Boyle JP, Grigg ME, Arrizabalaga G, Boothroyd JC (2005) Bioluminescence imaging of *Toxoplasma gondii* infection in living mice reveals dramatic differences between strains. *Infect Immun* 73(2):695–702.

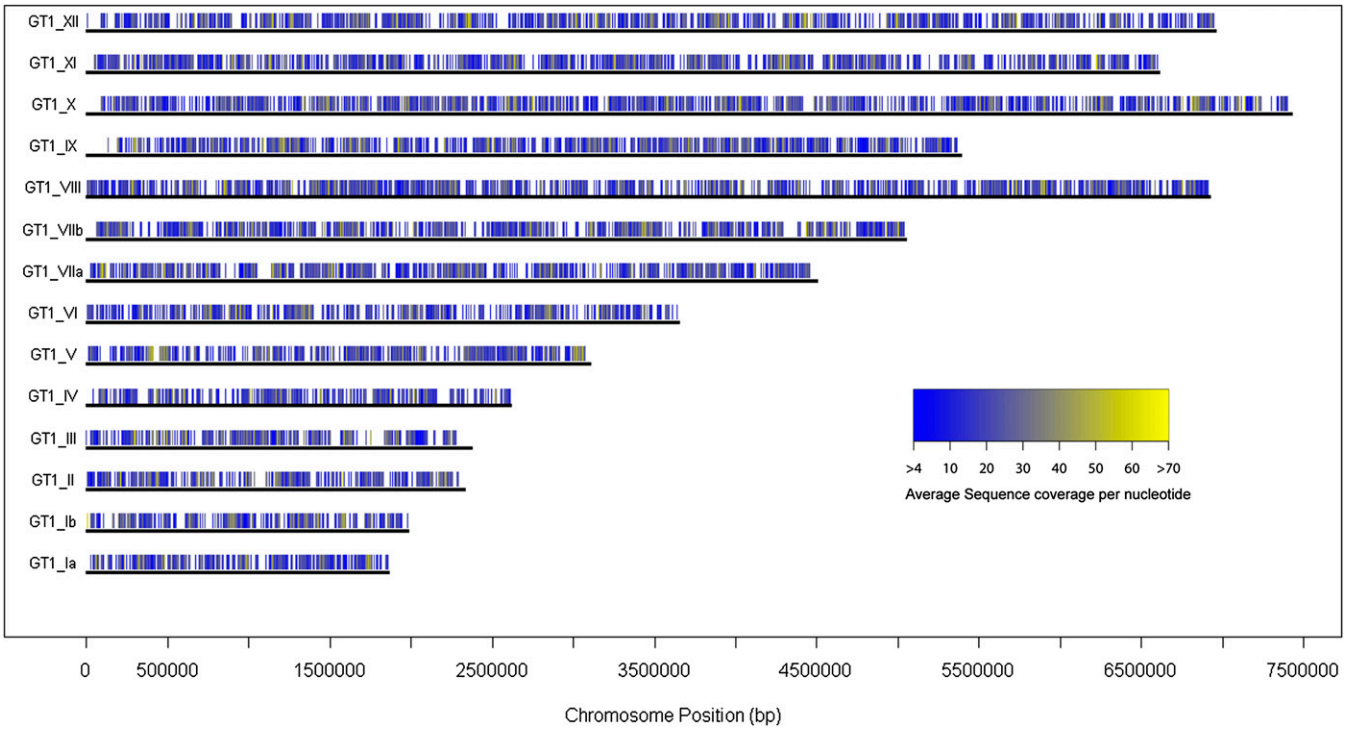

Fig. S1. Raw sequence coverage plot of sequence reads across the *T. gondii* GT1 genome. Heatmap indicates the overall level of sequence coverage in each 1,000-bp window. Windows with bars of any color had >3× coverage for ≥750 positions of the 1,000-bp window.

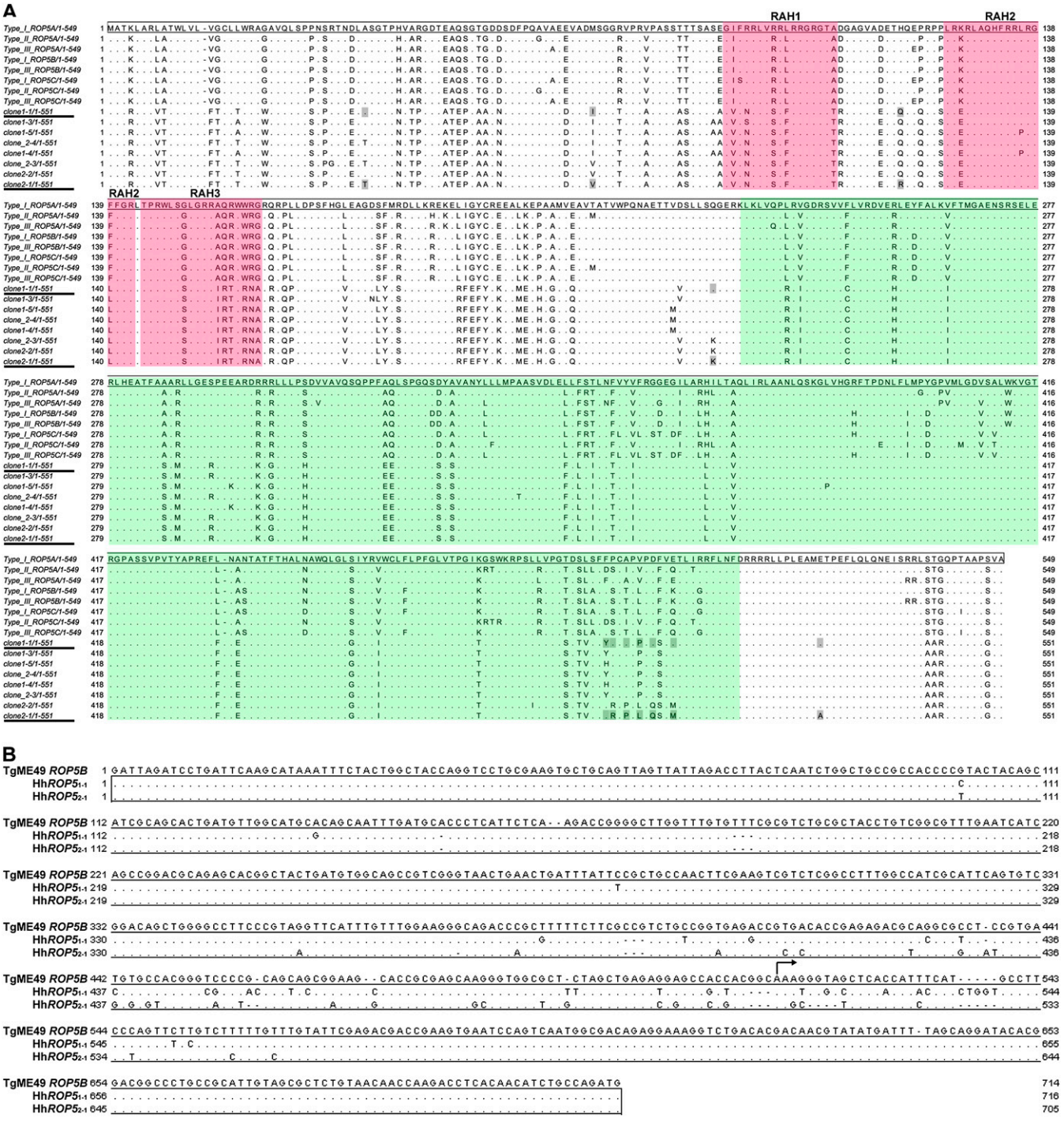

Fig. S2. Both *T. gondii* and *H. hammondi* harbor multiple distinct ROP5 paralogs. (*A*) ClustalW alignment of all known *H. hammondi* and *T. gondii* ROP5 orthologs. The three amphipathic helices involved in parasitophorous vacuole association are highlighted in red; the pseudokinase domain is highlighted in green. Isoforms 1–1 and 2–1 (the subject of the present study) are underlined, and all amino acid residues that are different between these isoforms are shaded in gray. (*B*) Alignment of the promoter sequences for *ROP5Hh*$_{1-1}$, *ROP5Hh* $_{2-1}$, and TgType II (ME49) *ROP5B*, which were used in the promoter assays presented in Fig. S3*A*. The predicted transcriptional start site is indicated by a black arrow.

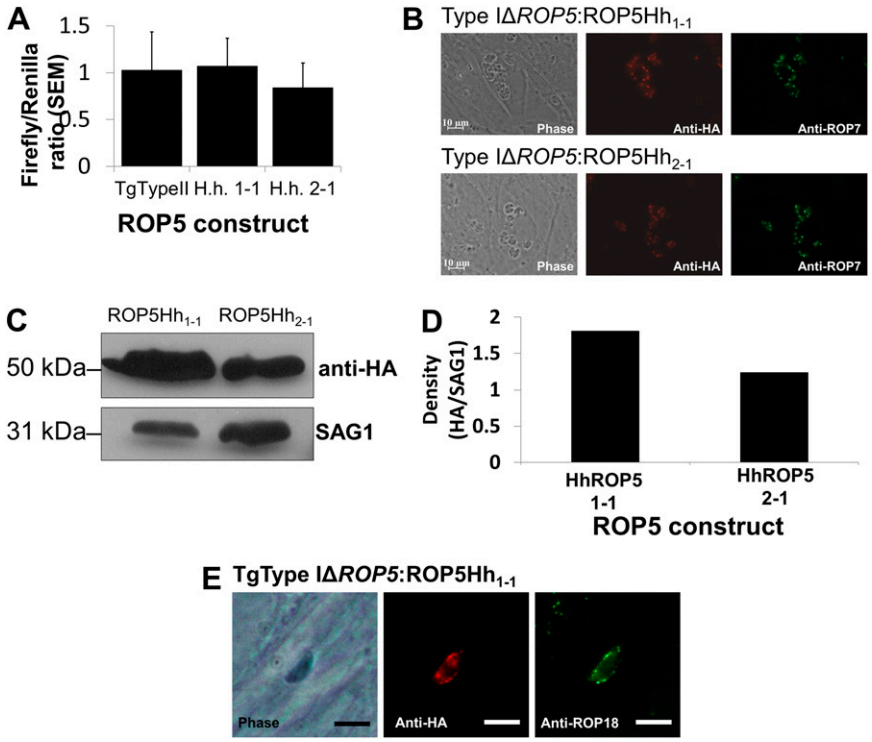

Fig. S3. HhROP5$_{1–1}$ and HhROP5$_{2–1}$ are trafficked to the *T. gondii* rhoptries and associated with the parasitophorous vacuole. (*A*) Promoter activity of upstream sequences from *TgROP5$_{II}$*, *HhROP5$_{1–1}$*, and *HhROP5$_{2–1}$* using dual luciferase assays. (*B*) Immunofluorscence showing the similar localization of HA-tagged HhROP5$_{1–1}$ and HhROP5$_{2–1}$ in *T. gondii* with the rhoptry marker ROP7 24 h postinfection. (*C*) Quantitative Western blotting of HA-tagged HhROP5$_{1–1}$ and HhROP5$_{2–1}$ using TgSAG1 as a loading control. (*D*) Quantification of data in Fig. S3*B* showing a slightly lower expression level for HhROP5$_{2–1}$ in *T. gondii* compared with HhROP5$_{1–1}$. (*E*) Immunofluorescence showing HhROP5$_{1–1}$ associating with the parasitophorous vacuole and colocalizing with TgROP18 4 h postinfection. Similar results were obtained for HhROP5$_{2–1}$.

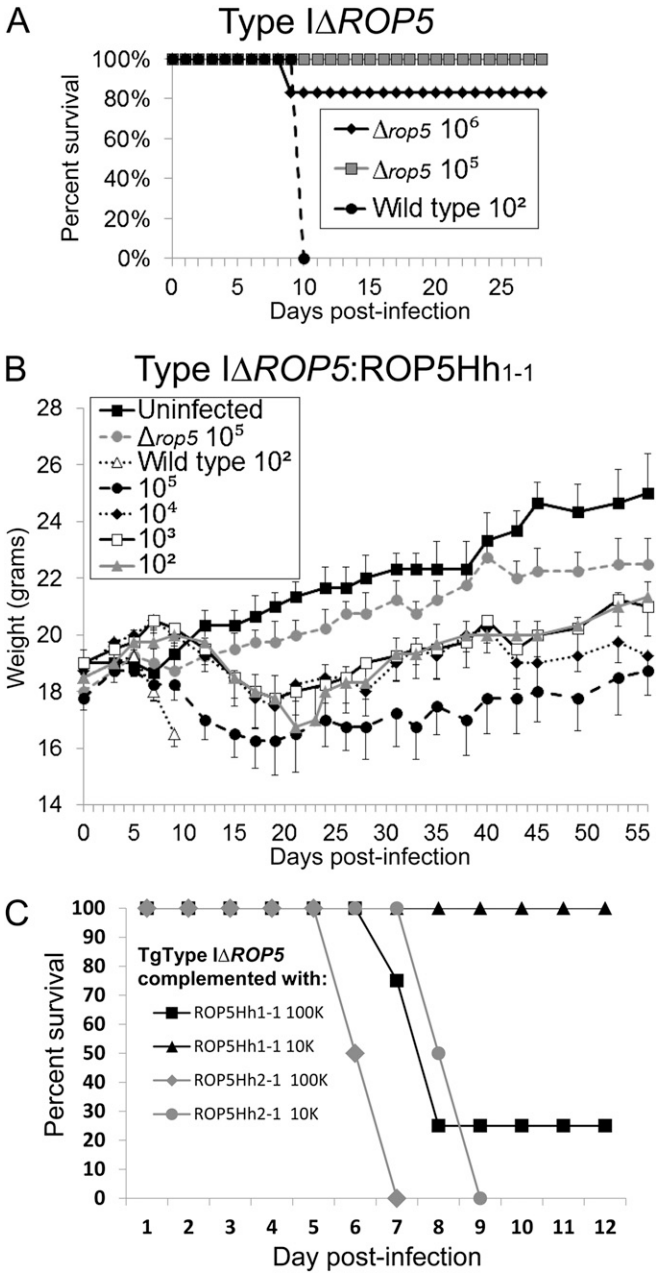

Fig. S4. HhROP5$_{1-1}$ and HhROP5$_{2-1}$ are not equivalent in their ability to increase the virulence of RHΔ*ROP5*. (*A*) Survival analysis of mice infected with RHΔ*ROP5* 10^6 ($n = 6$) and 10^5 ($n = 4$) along with RH 10^2 ($n = 4$) was used to reconfirm that the TgType I *ROP5* knockout is avirulent. (*B*) Mice infected with wild-type RH, RHΔ*ROP5*, or different doses of RHΔ*ROP5*:HhROP5$_{1-1}$ were weighed every 2–4 d to determine morbidity. Although in this experiment most mice infected with RHΔ*ROP5*:HhROP5$_{1-1}$ did not succumb to the infection, all lost weight compared with RHΔ*ROP5*-infected mice, particularly during the later stages of infection. (*C*) Genetically distinct clones expressing HhROP5$_{1-1}$ and HhROP5$_{2-1}$ (shown in Fig. 1 *B* and *C* and aligned in Fig. S2*A*) were compared in head-to-head infection experiments at the indicated doses. Whereas in this experiment more mice succumbed to infection with RHΔ*ROP5*:HhROP5$_{1-1}$ at doses as low as 10^4 tachyzoites, all mice infected with all doses of RHΔ*ROP5*:HhROP5$_{2-1}$ succumbed to the infection by day 9.

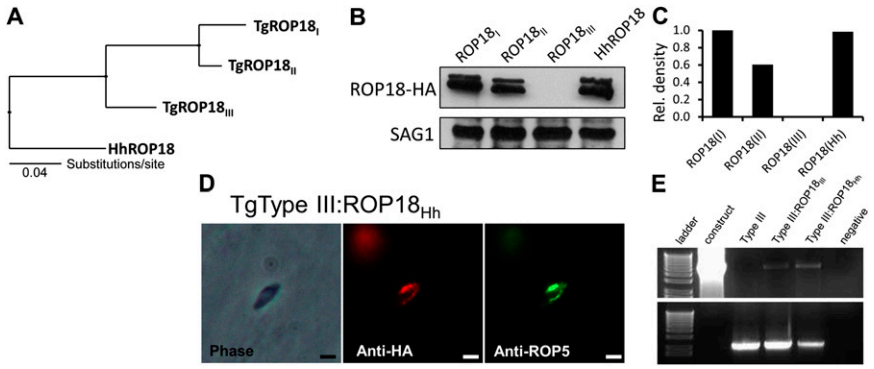

Fig. S5. (*A*) *H. hammondi* ROP18 is divergent from *T. gondii* ROP18 alleles from types I, II, and III but is most similar to *T. gondii* type III strain ROP18. Phylogram of amino acid ClustalW alignment of ROP18 orthologs from TgTypes I, II, and III and *H. hammondi*. (*B*) Quantitative Western blotting of HA-tagged orthologs of ROP18 (from types I, II and III *T. gondii* and *H. hammondi*) using surface antigen 1 (SAG1) as a loading control. (*C*) Quantification of the blot in Fig. S5*B* indicating similar expression between TgROP18$_{I}$ and HhROP18, slightly lower expression level of *T. gondii* type II ROP18, and undetectable expression for TgROP18$_{III}$ as expected. (*D*) Immunofluorescence showing HhROP18 associating with the parasitophorous vacuole and colocalizing with TgROP5 4 h postinfection. (*E*) PCR confirms the presence of the HA-tagged ROP18$_{III}$ construct in transfected parasites. HA-tagged ROP18$_{III}$ is not detectable in transfected parasites (Fig. 2*C*), and therefore PCR was used to confirm the presence of the construct containing the ROP18$_{III}$ insert (see Table S3 for primer sequences). The primers were made against the regions of the vector flanking the *TgROP18$_{III}$* or *HhROP18* insert (*Upper* half of gel) or against a known *T. gondii* genomic segment from chromosome II (*Lower* half of gel). Templates were as follows: lane 2 contained the plasmid construct, lane 3 contained type III strain genomic DNA, lane 4 contained DNA from a clone of type III parasites transfected with the *TgROP18$_{III}$*-containing vector, and lane 5 contained DNA from a clone of *T. gondii* type III parasites transfected with the *HhROP18*-containing vector. Lane 6 contains no DNA control.

Table S1. Raw genome sequencing data and assembly information for *Hammondia hammondi* HhCatGer041

Dataset	Parameter	
Illumina Paired End	Total reads*	61,274,250
	Size	36 bp
	Mean insert size	208 bp
	Stdev insert size	32 bp
	Total mapped reads[†]	36,272,770
PacBio (four SMRT cells)	Total consensus reads	3,524
	Mean size	1,462 bp
	Stdev[‡] size	431 bp
	Min size	5 bp
	Max size	2,606 bp
	Total mapped reads	3,309[§]

*Pairs included.
[†]Using Bowtie2 vs. *T. gondii* GT1 genome, v7.2.
[‡]standard deviation.
[§]BlastN vs. *T. gondii* GT1 genome, v7.2, expect $\leq 1e^{-20}$.

Table S2. Summary of *Hammondia hammondi* HhCatGer041 genomic assembly

	Contigs		Scaffolds	
Assembly	>100 bp	>500 bp	>100 bp	>500 bp
Number	63,731	20,269	56,472	15,313
N50	2,921	3,981	4,675	5,854
Largest	77,750	77,750	81,009	81,009
Total length, Mb	55.4	46.4	56.4	48.4

Table S3. Primers used in the present study and description of their purpose

Forward (5′-3′) primer	Reverse (5′-3′) primer	Purpose
GAGCGGCGCGCCGGTTAGATCCTGTG TCAAGCATAA	AGCTCCCGGGAGCGACTCCGGGCGCAG CAGTAGGTTG	Cloning *H. hammondi* ROP5 isoforms into pUPRT-HA
CACCCTCGTCGACCACACAGCTAA*	CTACGCGTAGTCCGGGACGTCGTACGGGT ATTCTGTTTGGTGGTGTCCCTGCT†	Cloning *H. hammondi* ROP18 into pENTR-D-Topo
CACCCTCGTCGACCACACAGCTAA*	CTACGCGTAGTCCGGGACGTCGTACGGGTA TTCTGTTTGTAGATGTTCCTGCT	Cloning *T. gondii* type III ROP18 into pENTR-D-Topo
CACCCTCGTCGACCACACAGCTAA*	TTGCATTCCTGCAACAAGAC	Checking for pGra-att-GRA2 with *T. gondii* type III ROP18 in transfected *T. gondii*
AAACGCTCTAGGACAGATGCTC	TATCCGCTCACAATTCCACACGCTATCAA GAGACACGAACAG	Positive control for *T. gondii* PCR
CACCGGTTAGATCCTGTGTCAAGCATAA*	ATCCATCTGGCAGTTTCAGTGAGGTCTG‡	Cloning the promoters of *H. hammondi* ROP5 isoforms into pENTR-D-Topo
CACCGATTAGATCCTGATTCAAGCATAA*	ATCCATCTGGCAGATGTTGTGAGGTCTT‡	Cloning the promoter of *T. gondii* type II ROP5 isoform into pENTR-D-Topo
CACCCTCGTCGACCACACAGCTAA*	ATCCATTCGGACGAGGGTACAAGCAAG‡	Cloning the promoter of *H. hammondi* ROP18 into pENTR-D-Topo
CACCCTCGTCGACCACACAGCTAA*	ATCCATTCGGACGACGGTACGCGTAA GAGGTGGC‡	Cloning the promoter of *T. gondii* type II ROP18 into pENTR-D-Topo
CACCCTCGTCGACCACACAGCTAA*	ATCCATTCGGACGACGGTACACGTAAGA GATGGC‡	Cloning the promoter of *T. gondii* type III ROP18 into pENTR-D-Topo
CACCCTCGTCGACCACACAGCTAA*	CGGTTGTATCAATCTGTCGAGCATGGC TTGAGTAGCCCAC	Left region of SOE§ PCR to delete 107 bp of *H. hammondi* ROP18 promoter
GTGGGCTACTCAAGCCATGCTCGACAGATTGATACAACCG	ATCCATTCGGACGAGGGTACAAGCAAG‡	Right region of SOE PCR to delete 107 bp of *H. hammondi* ROP18 promoter

*CACC is used at beginning of forward primer for directional cloning into Gateway entry vector pENTR/D-Topo (Invitrogen).
†CTACGCGTAGTCCGGGACGTCGTACGGGTA encodes, in antisense, an HA tag with stop codon.
‡ATCCAT encodes, in antisense, the start codon and an aspartic acid.
§Splicing by overlap extension PCR.

Table S4. Raw firefly and *Renilla* luciferase values for the promoter assays described in this manuscript and represented as ratios in Figs. 1*C* and 3*B*

	Rep. 1		Rep. 2		Rep. 3		Rep.4	
Construct	Firefly	*Renilla*	Firefly	*Renilla*	Firefly	*Renilla*	Firefly	*Renilla*
ROP18 promoter assays								
ROP18 graph 1 (Fig. 3*B*, *Left*)								
Type II	396,277	29,723	76,643	4,368	—	—	—	—
Type III	696	6,202	658	3,039	—	—	—	—
H. hammondi	138,748	12,623	55,949	4,087	—	—	—	—
H. hammondi Δ107bp	343	2,830	427	3,866	—	—	—	—
ROP18 graph 2 (Fig. 3*B*, *Right*)								
Type II	ND*	ND	1,134,848	4,273,115	1,184,654	3,662,101	—	—
Type III	3,148	611,927	11,856	4,174,514	21,378	3,260,277	—	—
H. hammondi	237,694	438,839	685,005	2,436,742	471,161	1,866,608	—	—
Type III + *H. hammondi* 107 bp	1,582,984	446,237	5,404,837	3,235,530	8,235,066	3,793,976	—	—
ROP5 promoter assays								
Fig. 1*C*								
Type II (ROP5B)	56,267	163,271	72,428	245,511	17,088	10,707	23,487	12,586
H. hammondi 1–1	135,784	253,963	49,201	79,610	16,757	12,136	21,796	12,442
H. hammondi 2–1	57,796	168,949	67,044	150,320	23,792	16,882	14,820	12,757

ND, not determined.

Other Supporting Information Files

Dataset S1 (XLSX)